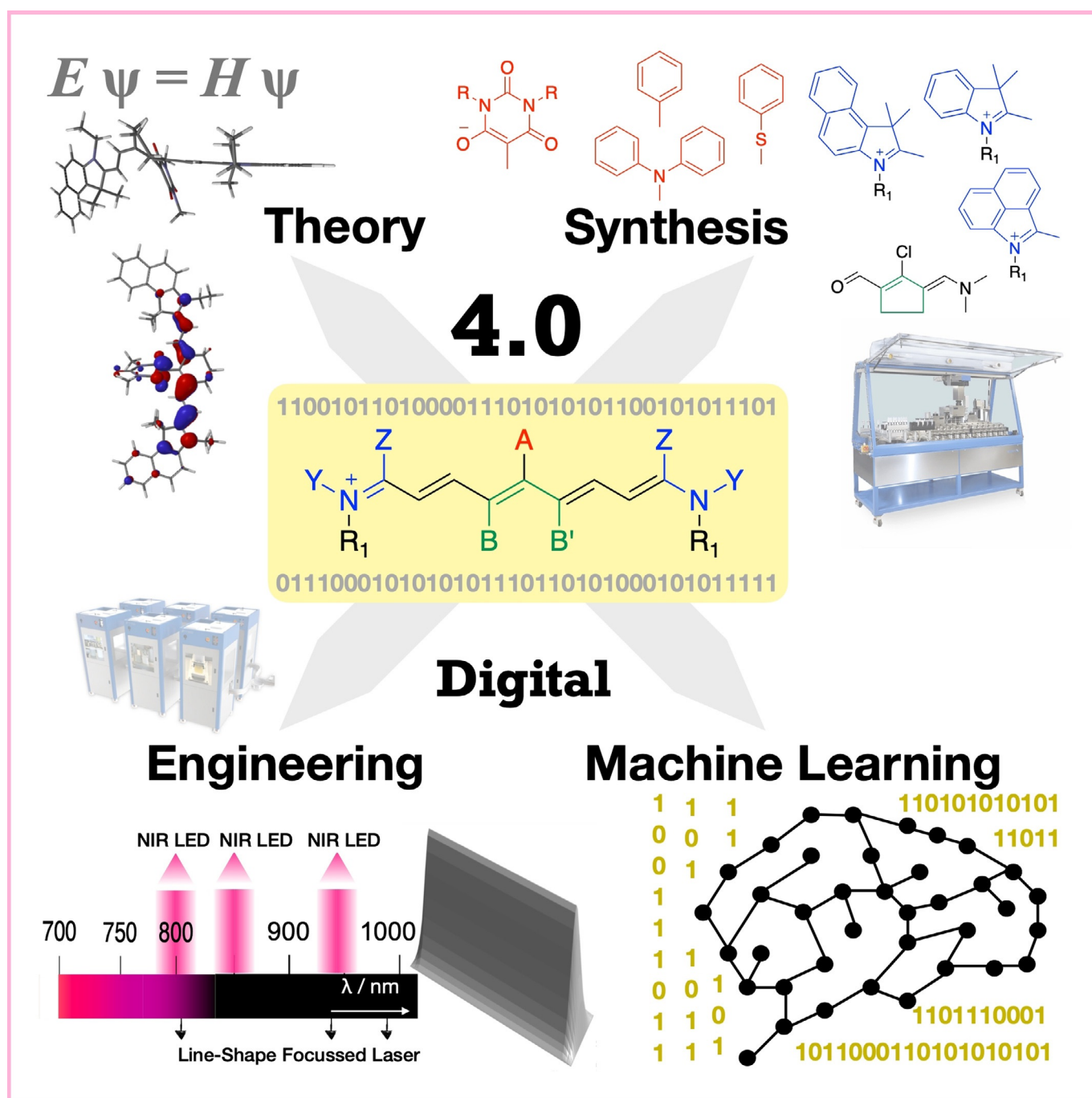


Artificial Intelligence | *Hot Paper* |

# Photochemistry with Cyanines in the Near Infrared: A Step to Chemistry 4.0 Technologies

Bernd Strehmel,<sup>\*,[a]</sup> Christian Schmitz,<sup>\*,[a]</sup> Kevin Cremanns,<sup>[b]</sup> and Jost Göttert<sup>[c]</sup>



**Abstract:** Cyanines covering the absorption in the near infrared (NIR) are attractive for distinct applications. They can interact either with lasers exhibiting line-shaped focus emitting at both 808 and 980 nm or bright high intensity NIR-LEDs with 805 nm emission, respectively. This is drawing attention to Industry 4.0 applications. The major deactivation occurs through a non-radiative process resulting in the release of heat into the surrounding, although a small fraction of radiative deactivation also takes place. Most of these NIR-sensitive systems possess an internal activation barrier to react in a photonic process with initiators resulting in the generation of reactive radicals and acidic cations. Thus, the heat released by the NIR absorber helps to bring the system, consisting of an NIR sensitizer and initiator, above such internal barriers. Molecular design strategies making these systems more compatible with distinct applications in a certain oleophilic surrounding are considered as a big challenge. This includes variations of the molecular pattern and counter ions derived from super acids exhibiting low coordinating properties. Further discussion focusses on the use of such systems in Chemistry 4.0 related applications. Intelligent software tools help to improve and optimize these systems combining chemistry, engineering based on high-throughput formulation screening (HTFS) technologies, and machine learning algorithms to open up novel solutions in material sciences.


## Introduction


Nowadays, the number of applications focusing on the use of NIR absorbers and sensitizers<sup>[1]</sup> has been growing in many areas.<sup>[2]</sup> Digital imaging applied in computer to plate (CtP)

[a] Prof. Dr. B. Strehmel, Dr. C. Schmitz  
Department of Chemistry and Institute for Coatings and Surface Chemistry  
Niederrhein University of Applied Sciences  
Adlerstr. 1, 47798 Krefeld (Germany)  
E-mail: bernd.strehmel@hsnr.de  
christian.schmitz@hsnr.de

[b] K. Cremanns  
Department of Mechanical Engineering  
Institute of Modelling and High-Performance Computing  
Niederrhein University of Applied Sciences  
Reinarzstr. 49, 47805 Krefeld (Germany)

[c] Prof. Dr. J. Göttert  
Department of Electrical Engineering and Computer Sciences  
HIT-Hochschule Niederrhein Institute of Surface Technology  
Niederrhein University of Applied Sciences  
Reinarzstr. 49, 47805 Krefeld (Germany)

 The ORCID identification number(s) for the author(s) of this article can be found under: <https://doi.org/10.1002/chem.201901746>.

 © 2019 The Authors. Published by Wiley-VCH Verlag GmbH & Co. KGaA. This is an open access article under the terms of Creative Commons Attribution NonCommercial-NoDerivs License, which permits use and distribution in any medium, provided the original work is properly cited, the use is non-commercial and no modifications or adaptations are made.

technology represents one modern application.<sup>[3]</sup> Direct patterning of lithographic plates for 2D printing becomes possible by using semiconductor lasers emitting at 830 nm. However, specially designed absorbers<sup>[3]</sup> are a prerequisite, having the capability to sensitize the generation of reactive intermediates such as radicals and/or stable acidic cations resulting in the initiation of radical and/or cationic crosslinking.<sup>[4,5]</sup> Laser welding,<sup>[6]</sup> laser drying of offset printing inks using temperature sensitive substrates such as paper,<sup>[7]</sup> laser marking of plastics<sup>[8]</sup> or thermal curing<sup>[9]</sup> can be seen as additional applications benefiting from the main property of the NIR-sensitive materials; that is the on-demand release of heat as the main deactivation route, turning reactions ON and/or OFF.<sup>[10]</sup>

Many NIR initiators absorbing between 750–850 nm result in a non-radiative deactivation of more than 85 %, whereas fluorescence decays for some examples in sub-ns time with < 15 % efficiency.<sup>[5,10c]</sup> Sometimes, fluorescence appeared only as traces, that is  $\ll 1\%$ .<sup>[5,11]</sup> Moreover, absorbers with  $\lambda_{\text{max}} > 900$  nm deactivate almost only non-radiative (> 99 %).<sup>[11]</sup> Although fluorescence occurs with less efficiency, there exists a probability for bimolecular reactions in the excited state having a lifetime in the sub-nanosecond time frame,<sup>[10c]</sup> that is photoinduced electron transfer resulting in the formation of reactive intermediates.<sup>[10c,11,12]</sup>

One benefit of NIR radiation is the deeper penetration of radiation into matter due to its lower scattering coefficients compared to UV radiation.<sup>[13]</sup> Furthermore, excitation occurs at an energy decoupled from the UV and visible range. This facilitates embedding of UV filter materials into coatings to protect them against solar weathering.<sup>[14]</sup> Additive manufacturing<sup>[15]</sup> including volumetric printing<sup>[16]</sup> additionally benefits from this technology in particular when the printing process requires embedded functional materials absorbing in the UV and/or visible range. This is also suitable for ceramics.<sup>[17]</sup>

Applications relying on NIR radiation depict a certain competition compared to well established UV or visible light-sensitive systems. Nevertheless, the latter exhibit a higher sensitivity because non-radiative deactivation resulting in release of heat is not the major pathway in either UV or visible light sensitive systems. Consequently, the release of heat relating to non-radiative deactivation promotes physical events such as melting of powder coatings,<sup>[9,10a]</sup> suggested as sustainable green technology. For comparison, UV curable powder coatings have been already available, but they still require thermal treatment in an oven<sup>[18]</sup> to melt the powder. This can be overcome with NIR-based systems, in which physical events (melting) and chemical reactions just occur in one step.<sup>[9,10a,b]</sup> They are also of more general interest for physical drying of aqueous dispersion in a short time offering the opportunity to replace undesired oven techniques by photonic sources resulting in ON/OFF heat sensitive systems. This has also opened up new patterning opportunities utilizing intense diode lasers exhibiting spatial modulation resulting in 2D exposure pattern.<sup>[3,10,11]</sup> Furthermore, extension of an exposure scan along the z-axis can facilitate 3D printing.

Since high-power NIR LEDs have complemented available radiation sources,<sup>[5]</sup> there is a growing demand for absorbers

and sensitizers for applications benefiting from NIR excitation. Requirements include i) absorption is matching with the emission spectrum of the radiation source, ii) material is compatible with the matrix material, and iii) a certain energy threshold allowing handling of this light sensitive material at moderate room light conditions. The latter depicts a challenge for industrial applications related to Chemistry 4.0.

## Chemistry 4.0

The term Chemistry 4.0 is following the concept of Industry 4.0 and the German association VCI ("Verband der Chemischen Industrie e.V.") describing its development over time starting with Chemistry 1.0.<sup>[19]</sup> The industrial revolution started in the 18th century by using fossil energy (coal) and chemical processes (firing) to generate mechanical power for industrial processes. In the 19th century the chemical industry began its first period called Chemistry 1.0, also known as founder's time or "Gründerzeit", heavily based on coal chemistry. Followed by petrochemistry using oil as raw material, Chemistry 2.0 brought scale up of production and new classes of materials such as polymers. Globalization and the production of fine chemicals have opened the doors to a new area of industrial chemistry in the early 1980s, that is Chemistry 3.0. In the last years, the growth of the internet as well as new hard- and software tools have shifted the focus to developing digital-based production technologies also named Chemistry 4.0. This digital revolution of the chemical industry is aiming for a sustainable recycling or circular economy using waste as renewable source or feedstock of new production cycles. By 2040, the global production volume of the chemical industry will almost double—digitalization will help to achieve these goals. It also includes the use of artificial intelligence—software tools learning from huge amounts of experimental data. A sub-group of this is machine learning—which allows an adaptive approach of the classical design of experiment (DoE).

Chemical systems responding to NIR radiation also fit in this concept.<sup>[2a,b,f,3]</sup> Fast replacement of energy-wasting light sources such as mercury lamps (requested by law in the EU) or thermal sources such as ovens, drive and support Chemistry 4.0 solutions. Exposure based on NIR sources also results in photochemical reactions controlling several parameters including emission range, intensity, exposure time, absorber concentration and their photonic properties. This also addresses the necessity to readjust well-examined systems.<sup>[2–7,9a,10,11]</sup>

High-throughput formulation screening (HTFS) represents one feasible opportunity for systematic study of chemical systems using advanced robotic systems.<sup>[20]</sup> Here, many experiments can be carried out under controlled and repeatable conditions providing valuable, good data. The automation, which still relates to Industry 3.0 standards, of radiative-sensitive formulations and exposure of them in the workflow shown in Figure 1 creates a data set based on hundred or more samples per day varying and identifying all key parameters crucial for processing and performance. Nevertheless, a classical design of experiments can easily fail due to inadequate choice of factors or variables and their value combinations. A more sophisticated

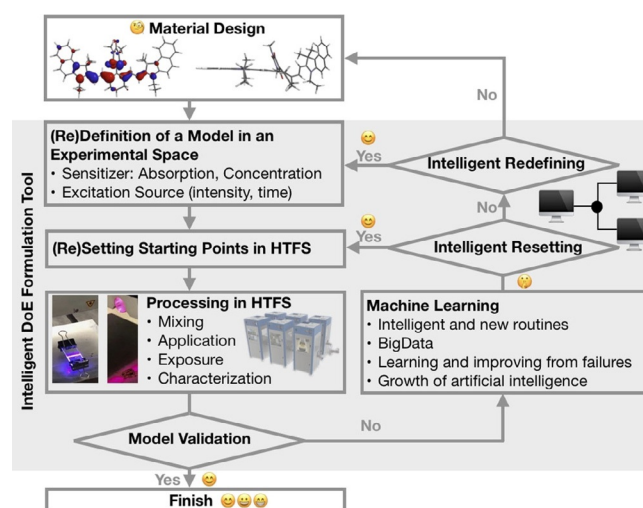


**Figure 1.** Workflow to design and process new materials in a setup based on an intelligent DoE to develop technologies.

approach is the use of machine learning algorithms running the analysis right on time, directly linked to the responses (measured output data) and suggesting new experiments based on the digital model uncertainty created from the actual data. Machine learning relates to Industry 4.0 standards to grow up artificial intelligence. Several approaches in theoretical chemistry<sup>[21]</sup> and engineering<sup>[22]</sup> have already started in this field to find new algorithms for optimizations of materials although both come from different fields.<sup>[21,22]</sup> Experimental studies complemented research in material sciences applying HTFS-techniques but with no application of machine learning algorithms.<sup>[20]</sup> Big improvements will be expected by combination of HTFS with machine learning in the near future.

In the future, machine learning algorithms will automatically control the HTFS equipment and stop the experimental process when the digital model reaches a certain prognosis quality threshold. This prognosis quality continuously improves by adding experiments, proposed by the machine learning algorithm. This drastically reduces the number of experiments and surpasses the classical DoE especially for large numbers of factors and responses. This combination of automation and machine learning results in a new methodology, which is called in this contribution "intelligent design of experiments" (iDoE).

Absorber parameters based on concentration, absorption, and geometry together with the radiation source providing both variable excitation wavelength and intensity importantly affect the overall performance of the system. Processing using HTFS equipment requires steps including mixing, application, exposure with either LED or laser, and characterization. All variables, parameter settings, and measured data train the digital model, which correlates input factors and characterization responses. Data analysis of this huge set of data is performed in a relatively short time with each experiment contributing to the model and improving it. A classical DoE would end at this point giving the information whether the experiment was successful or not. However, intelligent DoE uses advanced algorithms and iteratively improves the model and reduces its un-

certainty. This helps to predict results in a smaller confidence interval and improves the model facilitating to define new formulations with desired properties. This approach is generally referred to the field of artificial intelligence and big data sciences. Besides a general model of the chemical system, it is also possible to build a model predicting for example peak performance with regard to one specific attribute (optimization), or aiming for a robust formulation that is very tolerant to variations in the production cycle.<sup>[23]</sup> First trials of iDoE show promising results that will be published elsewhere.<sup>[22d]</sup>

## NIR Light as Reagent and Tool

Many efforts in photochemical sciences resulted in the development of new technologies representing a part of the entire technology.<sup>[24]</sup> 2D and 3D printing based on UV or visible light excitation depict some representative examples.<sup>[3,19]</sup> Moreover, cw-lasers emitting in the NIR facilitated easy spatial modulation enabling many applications in the graphic industry.<sup>[3,4]</sup> Using appropriate NIR absorbers/sensitizers opens up new directions for global control of manufacturing processes just by changing exposure intensity, that is remotely through internet.<sup>[23]</sup>

Nowadays, NIR light can be found in some applications.<sup>[2,3,6-8]</sup> This surprises since the development of NIR sources emitting in the range from 750 to 1000 nm also brings certain benefits. Representative sources are cw-lasers with emission at 808, 830, 940 and/or 980 nm.<sup>[2a-b,3c,9-11]</sup> They have received attraction for industrial uses, in which many repetitive steps address the demand of high process robustness and reliability.<sup>[3]</sup> Pulsed lasers are not considered as an option.

High-intensity NIR LEDs<sup>[5]</sup> emitting at 805 nm depict an alternative radiation source in the NIR. Recently, cyanines derived heptamethines, comprising indolenine as terminal group, demonstrated the feasible generation of radicals and the first cationic photopolymerization.<sup>[5]</sup> The LED provided a power density of  $1.2 \text{ W cm}^{-2}$  from 3.5 cm. The NIR radiation absorbed leads to both the release of heat and initiation of photochemical reactions as a result of non-radiative deactivation and photoinduced electron transfer (PET), respectively.<sup>[12]</sup> Particular generation of heat by light absorption overcomes the necessary internal activation barrier of PET in cyanine-based systems.<sup>[5]</sup> A main advantage is the handling of such NIR sensitive systems at ambient light conditions. Attempts to use traditional low-intensity NIR LEDs emitting with an intensity of  $< 100 \text{ mW cm}^{-2}$  failed<sup>[11]</sup> because they cannot facilitate the necessary exposure intensity moving the reaction across the internal activation barrier. Future developments of high-intensity NIR-LED sources focus on much stronger emitting sources. This also enables excitation of up-conversion nanoparticles (UCNPs) resulting in generation of UV light with NIR lasers.<sup>[25]</sup>

Such strong emitting sources also result in faster bleaching of the sometimes-greenish colored absorbers, whose absorption resides around 800 nm. Alternatively, spectral shift to higher wavelength, preferentially above 900 nm, facilitates to use fewer strong colored absorbers. From our best knowledge, the number of available NIR-sensitive components exhibiting an absorption maximum between 840–950 nm is very limited.

There is a need to develop more appropriate absorbers. The emission of NIR sources separates well from the absorption of additives whose absorption covers the UV and/or visible region, Figure 2. This enables to embed such materials in coatings for printing in 2D as well as 3D applications.

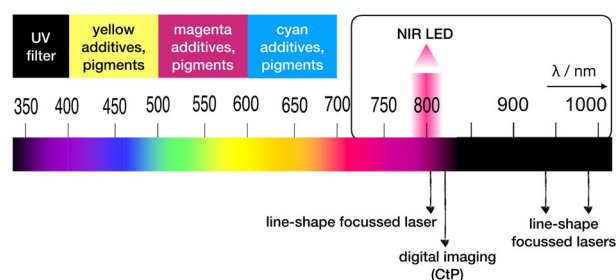


**Figure 2.** Schematic summary of the absorption for UV filter materials and additives covering the absorption in the visible range. They do not interfere the emission of NIR sources derived from LEDs with high emission intensity and NIR lasers used for manufacturing.

The fact that NIR-sensitive systems generate heat and reactive intermediates makes them attractive for technologies relying on physical and/or chemical processes.<sup>[9-11]</sup> Physical processes include melting of powder coatings as shown by treatment with lasers exhibiting line-shaped focus,<sup>[9-10]</sup> drying of aqueous dispersions as demonstrated for laser drying of offset printing inks<sup>[7]</sup> or drying of wet surfaces in general, Figure 3.

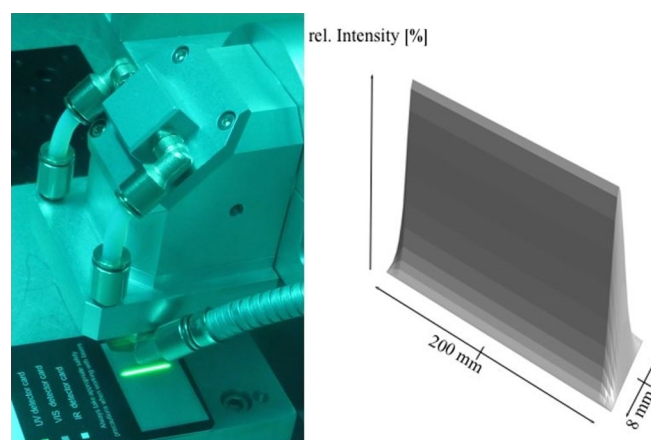


**Figure 3.** Laser with line-shaped focus (left) with emission at 808 and 980 nm and its intensity profile (right). An up-converting phosphorescent material visualized the laser light.

The heat released by the absorber in the deactivation process enables fast evaporation of volatile components with high spatial selectivity without the use of traditional furnace techniques. Chemical processes include generation of reactive intermediates resulting in crosslinking of monomers/prepolymers based on a thermal reaction<sup>[9]</sup> and/or a photonic mechanism.<sup>[5]</sup>

Nevertheless, NIR LEDs with very high exposure density can be seen as an alternative.<sup>[5]</sup> Figure 4 depicts the temperature of such a device released into the environment on the left



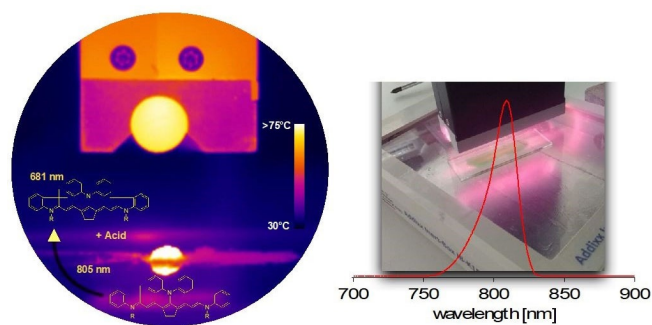


**Figure 4.** Temperature in the surrounding of a high power NIR LED (left). The absorber placed as powder depicts the hottest point. The right side depicts the spectrum emitted while a photopolymer composition was exposed.<sup>[5]</sup>

side, whereas the spectrum emitted is shown on the right side. The highest temperature is measured at the absorber applied as powder.

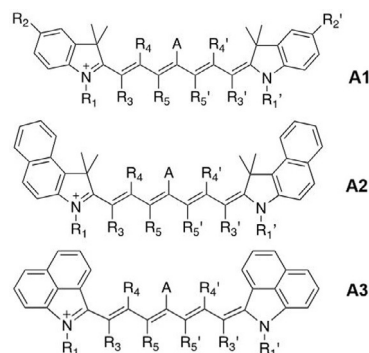
## NIR-Sensitive Components

Nowadays, several structural patterns of NIR absorbers were successfully introduced absorbing in the range from 700 to 1100 nm. This includes either cyanines,<sup>[1,2e-f,26]</sup> rylenes,<sup>[2f,27]</sup> porphyrines<sup>[2f]</sup> or conjugated polymers<sup>[2f]</sup>—just to mention a few of them.

Enough compatibility with the surrounding matrix used in the process is a challenge. Most of the aforementioned molecular approaches failed due to limited compatibility in practical systems (solubility, chemical stability), that is laser drying and CtP, in which cyanines and some rylenes showed the most promising practical performance.<sup>[2a,b,3,4,7,9-11,27]</sup> Nevertheless, undesired events such as H-aggregation and the aforementioned lower performance (solubility, crystallization under critical conditions, and shelf life in products caused by insufficient chemical stability) resulted in discontinuation of many promising industrial R&D projects.

Cyanines (**A1–A3**) may overcome some of these disadvantages. The substitution pattern uptakes a crucial function in this point. **A1–A3** can easily adjust the necessary absorber properties on demand for practical use. This includes introduction of bulky groups<sup>[2e-f,11]</sup> or distortion of planarity.<sup>[11]</sup> Bridging of  $R_5$  and  $R_5'$  with a  $\text{CH}_2$ -group results in a flexible cyclohexene moiety resulting in a distortion of planarity. This leads to an improved compatibility with the surrounding matrix.<sup>[11]</sup> On the other hand, direct bridging of  $R_5$  and  $R_5'$  results in a cyclopentene moiety. This keeps the conjugated backbone almost planar resulting in less compatibility with the surrounding matrix.<sup>[11]</sup>

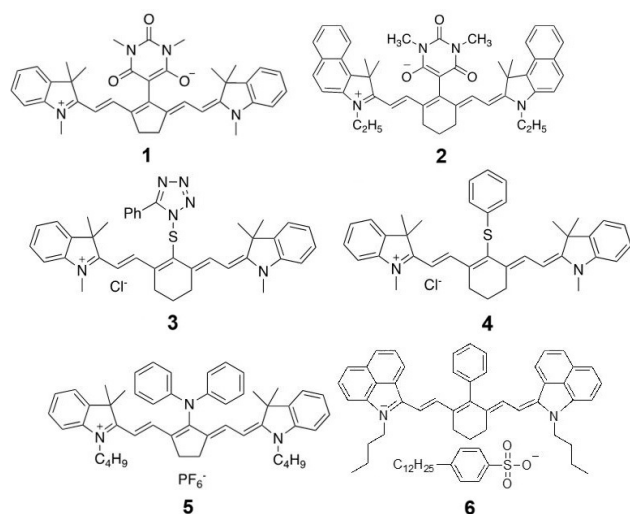
Bulky groups with large steric demand can be easily introduced with  $R_1$ .<sup>[11]</sup>  $R_3$ ,  $R_3'$ ,  $R_4$  and  $R_4'$  have been mostly presented by hydrogen. Replacement by alternative substituents might result in structures exhibiting a better photostability even under oxygen but the accessibility is limited by available procedures. The substituent **A** in the *meso*-position can exhibit



either electron-withdrawing or electron-donating properties resulting in the expected shift with no big changes of the redox potentials.<sup>[11]</sup> **A1–A3** can exhibit either a symmetric or an asymmetric pattern. The latter often improves compatibility with the surrounding matrix.

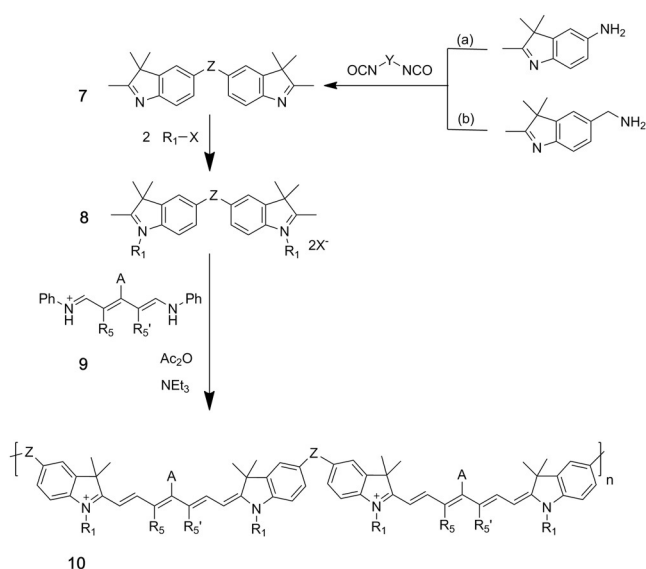
**1–6** represent some examples of **A1–A3** with potential for extension to more structures. **1–4** were successfully applied for negative digital imaging in CtP in which the  $R_i$  and  $R_i'$  form the structures shown. They differ regarding their absorption, whereas the redox potentials exhibit a rather modest change.<sup>[3,5,11]</sup> Surprisingly, the largest bathochromic absorption of about 200 nm occurred by exchanging the terminal group of either indolenine (**A1**) or benzindolenine (**A2**) with benzo-[*cd*]indolium moiety (**A3**)<sup>[5,11]</sup> while the number of unsaturated carbons in the polymethine chain remains the same. **6** worked excellently for laser drying of offset printing inks applying 980 nm laser radiation.<sup>[7]</sup> The respective counter ion resulted in a giant increase of solubility in organic solvents and monomers<sup>[11]</sup> facilitating the transfer to oleophilic printing inks.<sup>[7]</sup> Rylenes, although mentioned in patents,<sup>[7]</sup> were not able to compete with those cyanines. Future research might focus on cyanines with cationic structural pattern because the respective anion possesses more potential to affect absorber properties regarding compatibility compared to anionic absorbers bearing a cationic counter ion. On the other side, cyanines comprising  $\text{SO}_3^-$  groups exhibit enough water solubility while the net charge of the molecule depicts an overall negative charge. This transfers these absorbers to physical drying of aqueous dispersions applying the high-intensity LEDs and lasers with line-shaped focus mentioned in the previous section. In general, such combinations of absorbers and light sources also helps to get rid of old furnace techniques for drying technologies.

Comparison of solubility between the less planar absorbers such as **2–4**, and **6** with the more planar pattern shown in **1**, and **5** shows a huge increase of the solubility in reactive solvents by switching the geometry from a planar (**1**, **5**) to a distorted one (**2–4**, **6**). This was concluded considering structures **1** and **2**. Embedding of **1–6** in reactive solvents comprising acrylic groups showed acceptable compatibility with **2**, **5** and **6**.<sup>[11]</sup> As a result, change of the anion preferentially with those exhibiting low coordination properties and distortion of planarity of the conjugated system helps to improve the performance of NIR absorbers in industrial processing, in particular, to those related to Industry 4.0 standards.



The issue of incompatibility with a surrounding matrix is possible to overcome using an approach proposed for UV absorbers such as distyrylbenzenes comprising an alternating block pattern of aliphatic and conjugated moieties. This resulted in a polymer structure.<sup>[28]</sup> The amorphous material obtained exhibited a molecular weight of several kilo Daltons.<sup>[28]</sup> Thus, the final absorber becomes part of a polymer, which may help to solve the issue of migration, being critical for radiation curable printing inks used for food packaging.

Scheme 1 fits in this frame. Alkylation of **7** results in **8**, in which anion exchange improves the compatibility of the precursor with the surrounding matrix. **8** reacts with the chain builder **9** resulting in **10**. Following this approach, **Z** comprises urea moieties based on reasonable available starting materials carrying amino groups needed in step (a) or (b), respectively. Thus, a variation of **Y** results in a library of different precursors



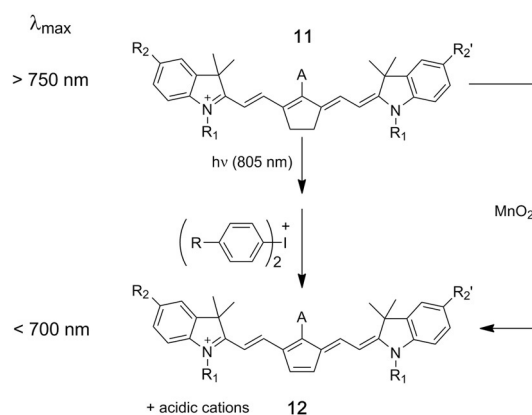
**Scheme 1.** Sketch for the synthesis of polymeric NIR sensitive materials comprising aliphatic block components to improve compatibility with many surroundings. This may occur according to ref. [28].

(**7**) exhibiting, depending on **Y**, variable properties of the final product **Y**.

A broad variety of absorbers has been proposed, although the choice for counter anions is not showing many variations. Halides, in particular chlorides, and tosylates were the most preferred anions. Dodecylbenzene sulfonate ( $C_{12}H_{25}-Ph-SO_3^-$ ) as introduced in **6** improved the solubility of this cationic absorber in oleophilic printing ink for laser drying.<sup>[7,11]</sup> Recently, bis(trifluoroalkyl)sulfonyl imides such as  $[(CF_3SO_2)_2N]^-$ <sup>[11,30]</sup> or aluminates such as  $[Al(O-t-C_4F_9)_4]^-$ <sup>[29]</sup> resulted in cationic absorbers with improved solubility in a variety of monomers used for radical and cationic polymerization.<sup>[5,29]</sup> These anions represent interesting alternatives compared to  $PF_6^-$ , which brings the issue of HF-release under certain conditions.<sup>[31]</sup> This has also brought the FAP-anion ( $[P(F_3C_2F_5)_3]^-$ ) as an alternative, resulting in materials exhibiting excellent compatibility with different oleophilic surroundings.<sup>[32]</sup> Anions derived from super acids may fit in this framework.<sup>[33]</sup>

Tetraphenyl borates  $[B(Ph)_4]^-$  were sometimes applied for NIR-sensitized radical polymerization.<sup>[3,10c]</sup> However, compatibility in solidified coatings limits its broader use.<sup>[3,10c]</sup> In addition, tetraphenylborate salts also showed a certain cytotoxicity,<sup>[30]</sup> whereas no issues have been reported about the comparable fluorinated material yet; namely,  $[B(PhF_3)_4]^-$ . This anion was introduced as an alternative in onium salts to improve their compatibility in different resins.<sup>[34]</sup> It possesses a high molecular mass, similar to  $[Al(O-t-C_4F_9)_4]^-$ ,<sup>[28]</sup> requiring a higher loading in the application if equimolar amounts would be requested. From this point of view, low molecular weight anions exist as alternatives; that is  $[(CF_3SO_2)_2N]^-$ ,<sup>[26]</sup>  $[(CF_3SO_2)_3C]^-$ <sup>[34]</sup> or  $[P(F_3C_2F_5)_3]^-$ .<sup>[31b,35]</sup>

Bridging of  $R_5$  and  $R_5'$  in **A1** led to the examples **1** and **5**. NIR exposure in the presence of **13** resulted in oxidation of the central moiety by PET and yielded a photoproduct exhibiting a hypsochromic shift of about 100 nm, Scheme 2.<sup>[5,36,37]</sup> This might surprise since **11** possesses an additional double bond in the conjugated backbone compared to **10**. Nevertheless, **10** belongs to cyanines, whereas **11** is partially a substituted fulvene. The chemistry of this reaction, however, still needs further examination. Color on demand applications may benefit



**Scheme 2.** Oxidation of NIR sensitizers with light and without light leads to fulvene type patterns.<sup>[5,36]</sup>

from this reaction because the final material appears deep blue, whereas the greenish color of the starting material disappeared. Future research will bring more impetus in this field.

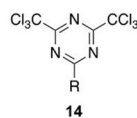
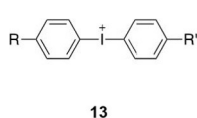
## Near Infrared Sensitive Materials with Internal Barrier

NIR sensitive materials used for sensitized generation of reactive intermediates follow a photoinduced electron transfer (PET), which often includes an internal activation barrier resulting in a system having a certain energy threshold. Equation (1) discloses the temperature dependence of the rate constant for electron transfer  $k_{et}$  in which the free activation enthalpy  $\Delta G_{et}^{\ddagger}$  determines the size of internal activation barrier.<sup>[12]</sup> This also requires knowledge about the free enthalpy of electron transfer ( $\Delta G_{et}$ ) and the reorganization energy  $\lambda$ .<sup>[12]</sup>

$$k_{et} = \nu_N \cdot \kappa \times \exp\left(-\frac{\Delta G_{et}^{\ddagger}}{RT}\right) = \nu_N \cdot \kappa \times \exp\left(-\frac{(\Delta G_{et} + \lambda)^2/4\lambda}{RT}\right) \quad (1)$$

( $\nu_N$ : theoretical maximal available rate,  $\kappa$ : probability coefficient).

Many NIR sensitive systems exhibit an internal activation barrier while  $\Delta G_{et} < 0$  using either an iodonium salt (**13**) or triazine (**14**) as acceptor. Experimentally, there is often no reaction under ambient light conditions, whereas strong sources such as lasers or high power NIR LEDs result in photochemical reactions. Thus, the positive charge of the absorber and the onium salt is likely not the reason for the internal activation barrier because **14** exhibits no charge. Both possess similar reduction potentials but the efficiency to initiate radical polymerization in combination with **2** was higher in the case of **13**.<sup>[11]</sup>



Crossing of the potential energy curves of the educts comprising the NIR sensitizer (**Sens**) and the acceptor (**13**) with those of the products **Sens<sup>++</sup>** and **13<sup>-</sup>**, respectively, obtained after electron transfer results in the scenario shown in Figure 5.<sup>[12]</sup> It demonstrates the necessity to introduce additional energy such as heat also under conditions in which  $\Delta G_{et} < 0$ . NIR-sensitive systems comprising sensitizers selected from either **A1**, **A2** or **A3** and an acceptor (**13** or **14**) possess  $\Delta G_{et}$  values being either slightly positive, neutral or slightly negative; that is  $\pm 0.5$  eV.<sup>[5,11]</sup> Outer sphere (dielectric constant of the surrounding) and inner sphere coordinates contribute to  $\lambda$ . This may reside between 1–1.5 eV.<sup>[12]</sup> Non-radiative deactivation of the NIR sensitizer being the main deactivation route additionally provides enough thermal energy to overcome the activation barrier. It can easily achieve temperatures  $> 120^\circ\text{C}$ .<sup>[9]</sup>

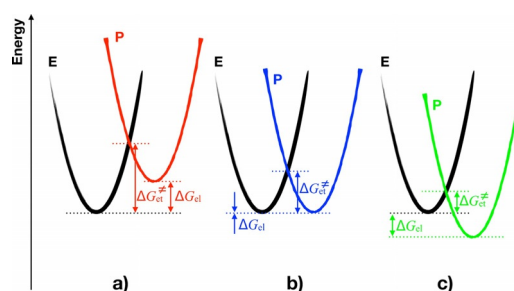
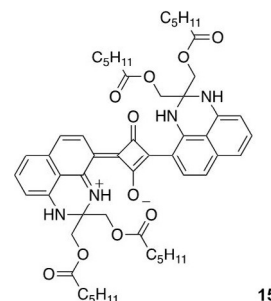


**Figure 5.** Energetic relations of photoinduced electron transfer with internal barrier resulting in threshold systems in which  $G_{et}$  is  $\pm 0.5$  eV. a) Endothermic conditions with  $G_{et}^{\ddagger}$  and  $G_{et} > 0$ . b) Thermoneutral conditions with  $G_{et} \approx 0$ . c) Exothermic conditions with  $G_{et} < 0$ .  $G_{et}^{\ddagger}$  is higher than zero in all cases explaining the internal barrier and, therefore, threshold of such systems.

Surprisingly, only a few of the absorbers showed chemical reactivity applying a low intensity ( $< 100 \text{ mW cm}^{-2}$ ) NIR-LED resulting in radicals and acidic cations.<sup>[11]</sup> They possess no net charge as shown for **1**, **2** or **15**. On the other hand, positively charged sensitizers (**3–6**) showed no reactivity with the aforementioned low intensity LED.<sup>[11]</sup> Switching the LED source to a device providing significant higher exposure intensity resulted in a remarkable reactivity of even positively charged sensitizers.<sup>[5]</sup> This helped the system to travel over an internal activation barrier. Moreover, it also facilitated the handling of such NIR sensitive materials under ambient room light conditions in which the formulations appeared as stable. This can be seen as a huge benefit in practical systems.



Future developments should also focus on systems resulting in less yellowing upon exposure in the presence of an acceptor. Some of the current systems absorbing around 800 nm shift their green color toward a strong yellow/brownish appearance.<sup>[38]</sup> Photoproducts formed cause this color, which limits their use for diverse applications.

Furthermore, the synthesis of new NIR absorbers may additionally focus on the availability of materials exhibiting a sufficient intersystem crossing, resulting in population of the triplet state. Nowadays systems operate from the first excited singlet state. Replacement of some hydrogens by heavy atoms in either **A1**, **A2** or **A3** improves accessibility to the triplet state. This easily prevents electron back transfer requiring no design of three-component systems.<sup>[3]</sup> Definitely, photodynamic

therapy would benefit from such materials due to the availability of NIR absorbers with the capability to form singlet oxygen.

## NIR Sensitizers for HTFS Intelligent Machine Learning

Figure 6 shows a general Scheme for the design of NIR sensitive materials used in applications related to Industry 4.0. It covers broad applicability starting from molecular properties

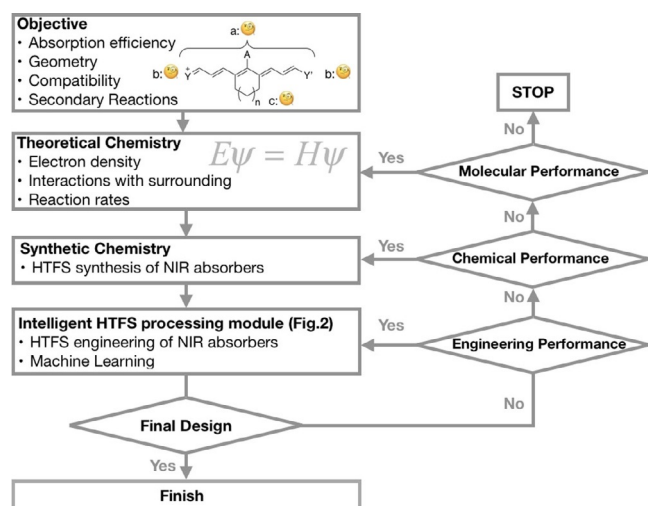


**Figure 6.** Combination of chemistry (theoretical and synthetic chemistry), engineering and informatics creating artificial intelligence results in intelligent tools for the development of new materials. NIR technology may benefit from these developments.

available by tools in theoretical chemistry, transfer of the best candidates to synthetic chemistry, although only a few of them will end in iDoEs (see Figure 1, applied in engineering). Machine learning helps to move the system in each direction. Only a combination of them results in fast success. This also includes the special example shown in Figure 6.

- 1) Tailor-made absorption by choosing the appropriate conjugation length, terminal group or substitution at the *meso*-position.
- 2) Establishing a molecular pattern with good compatibility in the surrounding matrix and negligible aggregation.
- 3) Tailor-made design of absorbers with an internal barrier enabling processing at ambient light conditions.
- 4) Secondary reactions as shown for example in Scheme 2 receive importance in color on demand applications.

Molecular design starts with molecular modeling to predict chemical properties of NIR-sensitized materials on the molecular scale. Molecular modeling provides a pattern for electron density, charge distribution, and reactivity. Theoretical chemistry introduced promising results for machine learning,<sup>[21a]</sup> in which for example kernel ridge regression was used to approximate the kinetic energy of non-interacting fermions in a one dimensional box as a function of their density. However, it

needed many samples to build this model because the advanced concept of iDoE was not used. Typically, the implemented algorithms learn from failure in DoE open up the feasibility to grow up artificial intelligence to enhance iDoE.

The initial results suggest combining molecular theory with HTFS-based synthesis to generate a library of materials along with a model of structural information related to application properties. Intelligent HTFS as shown in Figure 1 processes them to demonstrate the proper functionality for selected applications. In general, machine learning reduces the number of experiments required by ensuring that all proposed experiments provide a maximum amount of information.<sup>[22d]</sup> It also assures that the number of failed experiments is minimized and enhances therefore the efficiency of the R&D process.

The implemented algorithms autonomously reduce the number of factors from the theoretical prediction to the most important ones. This reduces the density of the possible design space and lowers the amount of required experiments to build an accurate model.

## Conclusions

Modern material research and development using advanced machine learning algorithms in conjunction with HTFS robotic tools will enhance:

- 1) The engineering performance by utilizing intelligent HTFS screening (Figure 1),
- 2) the chemical performance by reentering the synthesis HTFS module to understand the function of each moiety and the impact for the application (Figure 6), and
- 3) the molecular design process applying theoretical modeling thereby advancing the understanding of structure-property-relationship (Figure 6).

In the future, more special software tools will be needed to answer questions resulting from the combination of theoretical chemistry, synthetic chemistry, and molecular engineering of NIR sensitive materials in combination with HTFS processing. New machine learning algorithms, in part, will help to answer these questions. Intelligent HTFS together with modelling will result in best material and processing parameters using a minimum number of lab experiments. A major challenge will be the appropriate databases and handling/sharing of data. Although such HTFS systems possess the charm to pursue many experiments under well-defined conditions, the ultimate goal is to perform the least number of experiments to build the appropriate model of the chemical system investigated and use the model to predict the best formulation for a given application.

A first experiment to optimize a coating system using machine learning for color matching showed promising results.<sup>[22d]</sup> With more experiments planned it is likely that our results will start convincing the chemical community that many experiments as performed in classical HTFS experiments are not needed to build up a good model. In the future, intelligent HTFS will drive material research and development where arti-



ficial intelligence and machine learning will show with only a reasonably small number of experiments how molecular variations will result in the optimal formulations needed in an application.

## Acknowledgements

B.S. and J.G. acknowledge the project D-NL-HIT carried out in the framework of INTERREG-Program Deutschland–Nederland, which is co-financed by the European Union, the MWIDE NRW, the Ministerie van Economische Zaken en Klimaat and the provinces of Limburg, Gelderland, Noord-Brabant und Overijssel. B.S. and C.S. additionally thank the county of North Rhine–Westphalia for funding of the project REFUBELAS (grant 005-1703-0006). We also acknowledge Chemspeed Technologies AG for graphical material showing their automation modules in Figure 1 and in the Frontispiece.

## Conflict of interest

The authors declare no conflict of interest.

**Keywords:** absorber · artificial intelligence · chemistry 4.0 · near infrared · photochemistry

- [1] "Dyes, General Survey": H. Mustroph in *Ullmann's Encyclopedia of Industrial Chemistry*, Wiley-VCH, Weinheim, **2014**, pp. 1–35.
- [2] a) "NIR Light for Initiation of Photopolymerization": C. Schmitz, D. Oprych, C. Kutahya, B. Strehmel in *Photopolymerisation Initiating Systems* (Eds.: J. Lalevée, J.-P. Fouassier), Royal Society of Chemistry, Croydon, **2018**, pp. 431–478; b) "NIR-Dyes for Photopolymers and Laser Drying in the Graphic Industry": B. Strehmel, T. Brömme, C. Schmitz, K. Reiner, S. Ernst, D. Keil in *Dyes and Chromophores in Polymer Science* (Eds.: J. Lalevée, J.-P. Fouassier), Wiley, London, **2015**, pp. 213–249; c) A. H. Bonardi, F. Bonardi, F. Morlet-Savary, C. Dietlin, G. Noirbent, T. M. Grant, J. P. Fouassier, F. Dumur, B. H. Lessard, D. Gignes, J. Lalevée, *Macromolecules* **2018**, *51*, 8808–8820; d) A. H. Bonardi, F. Dumur, T. M. Grant, G. Noirbent, D. Gignes, B. H. Lessard, J. P. Fouassier, J. Lalevée, *Macromolecules* **2018**, *51*, 1314–1324; e) *Near-Infrared Dyes for High Technology Applications* (Eds.: S. Dähne, U. Resch-Genger, O. S. Wolfbeis), Springer, Netherlands, **1998**; f) Z. Y. Wang, *Near-Infrared Organic Materials and Emerging Applications*, CRC, Boca Raton, **2013**.
- [3] a) "Imaging Technology, 3. Imaging in Graphic Arts": H. Baumann, T. Hoffmann-Walbeck, W. Wenning, H.-J. Lehmann, C. D. Simpson, H. Mustroph, U. Stebani, T. Telsler, A. Weichmann, R. Studenroth in *Ullmann's Encyclopedia of Industrial Chemistry*, Wiley-VCH, Weinheim, **2015**, pp. 1–51; b) H. Baumann, *Chem. Unserer Zeit* **2015**, *49*, 14–29; c) B. Strehmel, S. Ernst, K. Reiner, D. Keil, H. Lindauer, H. Baumann, *Z. Phys. Chem.* **2014**, *228*, 129–153; d) B. Strehmel, H. Baumann, **2014**, Eastman Kodak Company, US8632937B2.
- [4] H. J. Timpe, *Materialwiss. Werkstofftech.* **2001**, *32*, 785–788.
- [5] C. Schmitz, Y. Pang, A. Gülz, M. Gläser, J. Horst, M. Jäger, B. Strehmel, *Angew. Chem. Int. Ed.* **2019**, *58*, 4400–4404; *Angew. Chem.* **2019**, *131*, 4445–4450.
- [6] a) M. R. Nakhaei, N. B. M. Arab, F. Kordestani, *Adv. Mater. Res.* **2012**, *445*, 454–459; b) F. Brunnecker, M. Sieben, *Laser Tech. J.* **2010**, *7*, 24–27; c) R. Wissemborski, R. Klein, *Laser Tech. J.* **2010**, *7*, 19–22; d) A. B. Humbe, P. A. Deshmukh, C. P. Jadhav, S. R. Wadgane, *Int. J. Pure Appl. Res. Eng. Technol.* **2014**, *2*, 191–206; e) S. Ernst, D. Keil, K. Reiner, B. Senns, **2018**, FEW Forschungs- und Entwicklungsgesellschaft Wolfen mbH, DE102016213372A1.
- [7] a) H. Pitz, **2003**, Heidelberger Druckmaschinen AG, EP 1302735 A2; b) D. Keil, H. Pitz, M. Schlörholz, **2008**, Heidelberger Druckmaschinen AG, DE102008028533A1; c) M. Schlörholz, **2012**, Heidelberger Druckmaschinen AG, DE102012017010A1; d) S. Ernst, G. D. Peiter, H. Pitz, K. Reiner, J. Mistol, M. Schlörholz, **2007**, Heidelberger Druckmaschinen AG, DE102008013312A1.
- [8] a) E. Pérez-Barrado, R. J. Darton, D. Guhl, *MRS Commun.* **2018**, *8*, 1070–1078; b) C. Patel, A. J. Patel, R. C. Patel, *Int. J. Sci. Res. Dev.* **2017**, *5*, 147–150; c) J. Loccufier, **2018**, Agfa-Gevaert N.V., WO2018228857A1; d) B. Waumans, I. Geuens, P. Callant, H. Van Aert, **2015**, Agfa-Gevaert N.V., US8975211B2; e) P. Callant, B. Waumans, **2015**, Agfa-Gevaert N.V., US20150261080A1; f) B. Waumans, P. Callant, I. Geuens, **2013**, Agfa-Gevaert N.V., EP2567825A1; g) B. Waumans, I. Geuens, P. Callant, H. Van Aert, **2012**, Agfa-Gevaert N.V., EP2463096A1; h) J. Thaker, **2011**, WO2011162814A2; i) M. Koenemann, A. Boehm, N. G. Pschirer, J. Qu, G. Mattern, **2007**, BASF Aktiengesellschaft, WO2007006717A1.
- [9] a) C. Schmitz, B. Strehmel, *J. Coat. Technol. Res.* **2019**, DOI: <https://doi.org/10.1007/s11998-019-00197-3>; b) C. Schmitz, B. Strehmel, *Eur. Coat. J.* **2018**, *124*, 40–44.
- [10] a) C. Schmitz, B. Strehmel, *ChemPhotoChem* **2017**, *1*, 26–34; b) C. Schmitz, B. Gökce, J. Jakobi, S. Barcikowski, B. Strehmel, *ChemistrySelect* **2016**, *1*, 5574–5578; c) T. Brömme, C. Schmitz, D. Oprych, A. Wenda, V. Strehmel, M. Grabolle, U. Resch-Genger, S. Ernst, K. Reiner, D. Keil, P. Lüs, H. Baumann, B. Strehmel, *Chem. Eng. Technol.* **2016**, *39*, 13–25.
- [11] C. Schmitz, A. Halbhuber, D. Keil, B. Strehmel, *Progr. Org. Coat.* **2016**, *100*, 32–46.
- [12] a) G. J. Kavarnos, N. J. Turro, *Chem. Rev.* **1986**, *86*, 401–449; b) N. J. Turro, V. Ramamurthy, J. C. Scaiano, *Principles of Molecular Photochemistry: An Introduction*, University Science Books, Sausalito, **2009**.
- [13] M. Uo, E. Kudo, A. Okada, K. Soga, Y. Jogo, *J. Photopolym. Sci. Technol.* **2009**, *22*, 551–554.
- [14] a) B. Strehmel, J. Moebius, S. Schäfer, C. Schmitz, T. Brömme, *Farbe Lack* **2012**, *118*, 25–30; b) T. Brömme, J. Moebius, S. Schäfer, C. Schmitz, B. Strehmel, *Eur. Coat. J.* **2012**, *9*, 20–27.
- [15] a) M. Singh, A. P. Haring, Y. Tong, E. Cesewski, E. Ball, R. Jasper, E. M. Davis, B. N. Johnson, *ACS Appl. Mater. Interfaces* **2019**, *11*, 6652–6661; b) B. Steyrer, P. Neubauer, R. Liska, J. Stampfl, *Materials* **2017**, *10*, 1445; c) A. Azizi, M. A. Daeumer, S. N. Schifres, *Addit. Manuf.* **2019**, *25*, 390–398.
- [16] B. E. Kelly, I. Bhattacharya, H. Heidari, M. Shusteff, C. M. Spadaccini, H. K. Taylor, *Science* **2019**, *363*, 1075–1079.
- [17] a) F. Bairo, I. Potestio, C. Vitale-Brovarone, *Materials* **2018**, *11*, 1524; b) E. Zanchetta, M. Cattaldo, G. Franchin, G. Brusatin, P. Colombo, M. Schwentenwein, J. Homa, P. Colombo, *Adv. Mater.* **2016**, *28*, 370–376; c) M. Schwentenwein, J. Homa, *Int. J. Appl. Ceram. Technol.* **2015**, *12*, 1–7.
- [18] R. Schwalm, *UV Coatings. Basics, Recent Developments and New Applications*, Elsevier, Oxford, **2007**.
- [19] More about Chemistry 4.0 can be found in "Growth through innovation in a transforming world" published by Verband der Chemischen Industrie VCI, **2017**. <https://www.vci.de/vci-online/services/publikationen/broschueren-faltblaetter/vci-deloitte-study-chemistry-4-dot-0-short-version.jsp>.
- [20] a) R. Hoogenboom, M. A. R. Meier, U. S. Schubert, *Macromol. Rapid Commun.* **2003**, *24*, 15–32; b) R. A. Potyrailo, B. J. Chrisolm, D. R. Olson, M. J. Brennan, C. A. Molaison, *Anal. Chem.* **2002**, *74*, 5105–5111; c) S. Schmatloch, H. Bach, R. A. T. M. von Bethem, U. S. Schubert, *Macromol. Rapid Commun.* **2004**, *25*, 95–107; d) D. C. Webster, *JCT Coatings-Tech* **2005**, *2*, 24–29.
- [21] a) M. Rupp, *Int. J. Quantum Chem.* **2015**, *115*, 1003–1005. This opens the special issue "Machine Learning and Quantum Mechanics Pages" in which many contributions show how new algorithms find fast solutions in chemistry with tools of theoretical chemistry. b) T. Lelièvre, G. Stoltz, *Acta Numer.* **2016**, *25*, 681; c) L. Li, T. E. Baker, S. R. White, K. Burke, *Phys. Rev. B* **2016**, *94*, 245129; d) L. Grajciar, C. J. Heard, A. A. Bondarenko, M. V. Polynski, J. Meeprasert, E. A. Pidko, P. Nachtigall, *Chem. Soc. Rev.* **2018**, *47*, 8307–8348.
- [22] a) K. Cremanns, D. Roos. "Deep Gaussian covariance network" arXiv:1710.06202, October **2017**; b) K. Cremanns, D. Roos, S. Hecker, A. Penkner, C. Musch, *Print Proceedings of the ASME Turbo Expo 2018: Turbomachinery Technical Conference and Exposition (GT2018)*, Vol. 8, ASME, New York, **2018**, V008T29A008; c) K. Cremanns, D. Roos, A. Penkner, S. Hecker, C. Musch, *Print Proceedings of the ASME Turbo Expo 2018: Turbo-*

- machinery *Technical Conference and Exposition (GT2018)*, Vol. 8, ASME, New York, **2018**, V008T29A007; d) C. Schmitz, K. Cremanns, L. Wagner, *Farbe Lack* **2019**, in press.
- [23] a) L. Plümer, P. Korolik, D. Koifman, H. Baumann, **2011**, Eastman Kodak Company, US20110189611A1; b) L. Plümer, P. Korolik, D. Koifman, H. Baumann, B. Strehmel, **2011**, Eastman Kodak Company, WO2011094243A1.
- [24] *Applied Photochemistry* (Eds.: R. Evans, P. Douglas, H. D. Burrow), Springer, Dordrecht, **2013**.
- [25] a) Z. Chen, D. Oprych, C. Xie, C. Kutahya, S. Wu, B. Strehmel, *ChemPhotoChem* **2017**, *1*, 499–503; b) Z. Chen, X. Wang, S. Li, S. Liu, H. Miao, S. Wu, *ChemPhotoChem* **2019**, DOI: <https://doi.org/10.1002/cptc.201900007>.
- [26] a) H. Mustroph, K. Reiner, J. Mistol, S. Ernst, D. Keil, L. Hennig, *ChemPhys-Chem* **2009**, *10*, 835–840; b) M. Halik, H. Hartmann, *Chem. Eur. J.* **1999**, *5*, 2511–2517; c) S. Ernst, J. Mistol, B. Senns, L. Hennig, D. Keil, *Dyes Pigm.* **2018**, *154*, 216–228; d) J. Fabian, H. Nakazumi, M. Matsuoka, *Chem. Rev.* **1992**, *92*, 1197–1226; e) H. Mustroph, A. Towns, *ChemPhys-Chem* **2018**, *19*, 1016–1023; f) H. Mustroph, K. Reiner, B. Senns, *Color. Technol.* **2017**, *133*, 469–475; g) L. Strekowski, M. Lipowska, G. Patonay, *Synth. Commun.* **1992**, *22*, 2593–2598.
- [27] a) Z. Yuan, S.-L. Lee, L. Chen, C. Li, K. S. Mali, S. De Feyter, K. Müllen, *Chem. Eur. J.* **2013**, *19*, 11842–11846; b) M. Koenemann, A. Boehm, N. G. Pschirer, J. Qu, G. Mattern, **2007**, BASF Aktiengesellschaft, WO2007006717A1.
- [28] a) A. M. Sarker, B. Strehmel, D. C. Neckers, *Macromolecules* **1999**, *32*, 7409–7413; b) B. Strehmel, H. Baumann, U. Dwars, D. Pietsch, A. Draber, M. Mursal, **2006**, Kodak Polychrome Graphics GmbH, DE102004055733B3.
- [29] A. Kocaarslan, C. Kütahya, D. Keil, Y. Yagci, B. Strehmel, unpublished results.
- [30] T. Brömme, D. Oprych, J. Horst, P. S. Pinto, B. Strehmel, *RSC Adv.* **2015**, *5*, 69915–69924.
- [31] a) J. G. Huddleston, A. E. Visser, W. M. Reichert, H. D. Willauer, G. A. Broker, R. D. Rogers, *Green Chem.* **2001**, *3*, 156–164; b) M.-C. Tseng, Y.-M. Liang, Y.-H. Chu, *Tetrahedron Lett.* **2005**, *46*, 6131–6136.
- [32] a) Y. S. Vygodskii, D. A. Sapozhnikov, A. S. Shaplov, E. I. Lozinskaya, N. V. Ignat'ev, M. Schulte, P. S. Vlasov, I. A. Malyshkina, *Polym. J.* **2011**, *43*, 126–135; b) N. D. Ignatyev, A. D. Kucheryna, U. D. Welz-Biermann, H. P. D. Willner, **2005**, Merck, DE10357360 A1.
- [33] A. Kütt, T. Rodima, J. Saame, E. Raamat, V. Mäemets, I. Kaljurand, I. A. Koppel, R. Y. Garlyauskayte, Y. L. Yagupolskii, L. M. Yagupolskii, E. Bernhardt, H. Willner, I. Leito, *J. Org. Chem.* **2011**, *76*, 391–395.
- [34] a) F. Castellanos, J. P. Fouassier, C. Priou, J. Cavezzan, *J. Appl. Polym. Sci.* **1996**, *60*, 705–713; b) F. Castellanos, J. Cavezzan, J.-P. Fouassier, C. Priou, **1993**, Rhône-Poulenc, EP0562897 A1.
- [35] A. Shiraishi, H. Kimura, D. Oprych, C. Schmitz, B. Strehmel, *J. Photopolym. Sci. Technol.* **2017**, *30*, 633–638.
- [36] a) Y. Iwai, K. Kunita, **2007** Fujifilm Corporation, US20070212643A1; b) Y. Iwai, K. Kunita, **2007** FUJIFILM Corporation, EP1849836 A2.
- [37] R. S. Lepkowicz, C. M. Cirloganu, J. Fu, O. V. Przhonska, D. J. Hagan, E. W. Van Stryland, M. V. Bondar, Y. L. Slominsky, A. D. Kachkovski, *J. Opt. Soc. Am. B* **2005**, *22*, 2664–2685.
- [38] T. Brömme, C. Schmitz, N. Moszner, P. Burtscher, N. Strehmel, B. Strehmel, *ChemistrySelect* **2016**, *1*, 524–532.

---

Manuscript received: April 15, 2019  
 Revised manuscript received: June 30, 2019  
 Accepted manuscript online: July 3, 2019  
 Version of record online: August 21, 2019